U.S. Fish & Wildlife Service

Arcata Fisheries Technical Report Number TR 2019-38

Estimating Annual *Ceratonova shasta* Mortality Rates in Juvenile Scott and Shasta River Coho Salmon that Enter the Klamath River Mainstem

Nicholas A. Som[1], Nicholas J. Hetrick[1], Russell W. Perry[2], and Julie D. Alexander[3]

[1]U.S. Fish and Wildlife Service
Arcata Fish and Wildlife Office
Arcata, California 95521

[2]U. S. Geological Survey
Western Fisheries Research Center
Columbia River Research Laboratory
Cook, WA 98605

[3]Oregon State University
Department of Microbiology
Bartholomew Lab
Corvallis, OR 97331

September 2019

Funding for this study and its supporting data collections was provided by a variety of sources, including the Klamath River Fish Habitat Assessment Program administered by the Arcata Fish and Wildlife Office, U. S. Fish and Wildlife Service Arcata Fish and Wildlife Office, U. S. Bureau of Reclamation, Klamath Falls Area Office, and NOAA Fisheries, California Coastal Office.

The Arcata Fish and Wildlife Office Fisheries Program reports its study findings through two publication series. The Arcata Fisheries Data Series was established to provide timely dissemination of data to local managers and for inclusion in agency databases. The Arcata Fisheries Technical Reports publishes scientific findings from single and multi-year studies that have undergone more extensive peer review and statistical testing. Additionally, some study results are published in a variety of professional fisheries journals.

key words: Coho Salmon, *Ceratonova shasta*, Juvenile, Klamath River, Mortality

The correct citation for this report is:

Som, N. A., N. J. Hetrick, R. W. Perry, and J. D. Alexander. 2019. Estimating annual *Ceratonova shasta* mortality rates in juvenile Scott and Shasta River Coho Salmon that enter the Klamath River mainstem. U.S. Fish and Wildlife Service. Arcata Fish and Wildlife Office, Arcata Fisheries Technical Report Number TR 2019-38, Arcata, California.

Table of Contents

List of Tables

List of Figures

Estimating Annual *Ceratonova shasta* Mortality Rates in Juvenile Scott and Shasta River Coho Salmon that Enter the Klamath River Mainstem

Nicholas A. Som[1,*], Nicholas J. Hetrick[1], Russell W. Perry[2], and Julie D. Alexander[3]

[1]U.S. Fish and Wildlife Service, Arcata Fish and Wildlife Office
1655 Heindon Road; Arcata, California

[2]U.S. Geological Survey, Western Fisheries Research Center
Columbia River Research Laboratory
5501A Cook-Underwood Rd; Cook, Washington

[3]Oregon State University, Department of Microbiology
Nash Hall 226; Corvallis, Oregon

[*]Corresponding author
nicholas_som@fws.gov

*Abstract.*The impacts of *Ceratonova shasta* on Klamath River salmonids have been the focus of tremendous research and monitoring over the past decade. Knowledge gained from the various studies has resulted in a growing suite of decision support tools that can be used to predict the prevalence of infection and mortality that can be expected from varying exposure concentrations to *C. shasta* waterborne spores, exposure durations, and water temperatures. More recent efforts have shown that when coupled with estimates of abundance and temporal migration timing, these tools can be used to predict population-level rates of annual mortality due to ceratomyxosis. In this report, we apply those tools to estimate annual mortality rates of juvenile Coho Salmon *Oncorhynchus kisutch* originating from the Scott and Shasta rivers that result from exposure to *C. shasta* in the mainstem Klamath River. Additionally, we simulate how a water management flow regime targeted to reduce disease risk may translate into differing estimates of mortality rates. In general, we found large variation among annual mortality rate estimates, ranging from 0% to 68% across both rivers and across all years considered in this investigation. Further, we estimate that fish from the Shasta River experienced higher mortality rates owning to their prolonged exposure history. Finally, our simulations suggest that the flow regime targeting reduced disease risk could be effective at reducing annual Coho Salmon mortality rate estimates, with the extent of the estimated reductions related to the timing of the onset of measurable in-river waterborne spore concentrations and the overlap with the Klamath River residence for each source population.

Background

Ceratomyxosis, the disease caused by the myxosporean parasite *Ceratonova shasta*, has led to increased mortality in Klamath River salmonids (Fujiwara et al. 2011), and the risk of mortality varies according to environmental variables including the waterborne concentrations of the parasite and water temperatures (Ray et al. 2014). While native salmonids exposed to low doses of the parasite exhibit some degree of resistance (Ching and Munday 1984; Bartholomew et al. 2001), they can become overwhelmed by high exposure levels that cause mortality (Bartholomew 1998; Stone et al. 2008). The parasite *C. shasta* is endemic to the Klamath Basin and assumed to have co-evolved with the salmonid species it infects. Coevolution over long periods of time often results in low virulence parasites that are in dynamic equilibrium with their hosts, assuming continued environmental variation under which this equilibrium evolved (Toft and Aeschilimann 1991; Esch and Fernandez 1993). When environmental variation significantly changes, the shift frequently favors the parasites pathogens given their shorter generation times and greater genetic variation than expressed in the hosts (Webster et al. 2007). In general, the pathogen adapts more quickly to environmental change than the host, causing the parasite-host equilibrium to unravel (Thompson 1994). This imbalance can be expressed as an elevated prevalence of host infections over naturally-occurring background or equilibrium levels, which is consistent with the abnormally high infection levels observed in juvenile salmon in the Klamath River during some years.

Recent work has supported the hypothesis that disease risk may be reduced by disturbance events that interrupt and limit the sustained temporal suitability of habitats for polychaete worms *Manayunkia speciosa* (Alexander et al. 2016), which are a host intermediate to salmonids in the *C. shasta* lifecycle. Hence, it has been further hypothesized that a water management flow regime that includes discharge events of sufficient magnitude and duration to disrupt the polychaete lifecycle and dependent habitats might lead to lower rates of *C. shasta* related mortality. Coho Salmon are among the species of salmonids that use the Klamath River mainstem each year, and their risk of infection and mortality due to *C. shasta* is of elevated concern given their protected status under the Endangered Species Act (ESA). Annual estimates of *C. shasta*-induced mortality rates are required to both quantify the population-level impacts, and to evaluate potential disease mitigation strategies. This report outlines the methods and results arising from an effort to address both components.

Methods

In this analysis, we estimate the proportions of Coho Salmon populations emigrating from the Shasta River and the Scott River that die from ceratomyxosis on an annual basis, which we define as the prevalence of mortality (POM). The POM computational methods presented herein generally track those outlined in Som et al. (2016b), in that weekly estimates of disease risk are integrated over the timing and cumulative exposure of an emigrating fish population to estimate POM for each year. However, Som et al. (2016b) estimated risk associated with *C. shasta* infections, whereas in this study we focus on estimating the risk of mortality, which cannot be assumed for all infected fish (True et al. 2017). We applied some methods of Ray et al. (2014) to a more contemporary, extended-sentinel trial dataset (USFWS, USGS, OSU, unpublished data) to estimate the parameters of a model for predicting mortality risk given a set of environmental variables. Parameter estimates from this model combined with observed or simulated environmental variables (details below) allow us to predict the proportion of fish that become diseased and eventually die from ceratomyxosis. Next, these model predictions were coupled with weekly-stratified abundance estimates of Coho Salmon passing through the monitoring stations on the Shasta and Scott rivers near their confluences with the Klamath River (e.g., Chesney and Knechtle 2016), yielding estimated weekly proportions of the Coho Salmon from those sources that emigrate through the infectious zone of the mainstem Klamath River and succumb to disease. We define the infectious zone as the mainstem Klamath River between the confluences of the Shasta River and Seiad Creek (Figure 1), noting that juveniles entering from the Scott River are only exposed between this confluence and Seiad Creek.

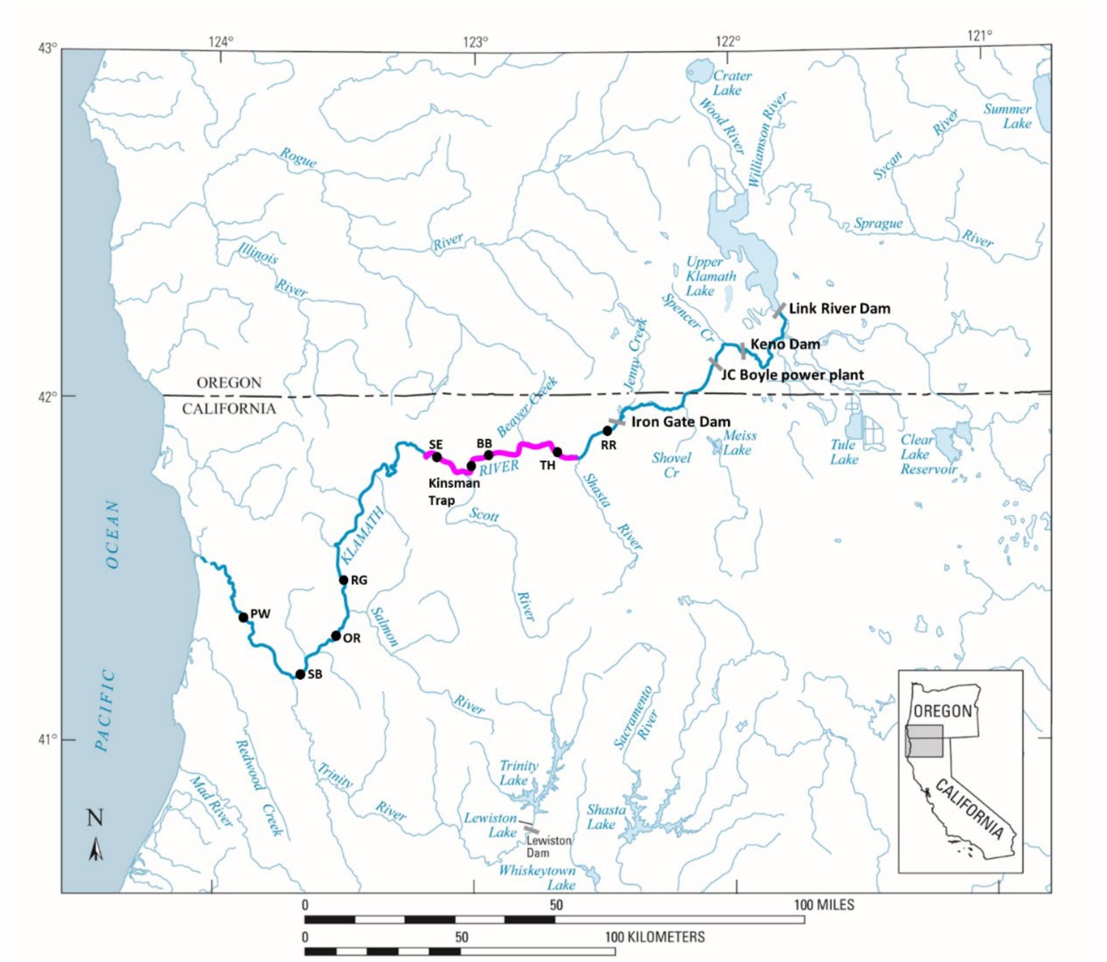

Figure 1. Klamath River map showing locations of major tributaries, dams, the Kinsman fish trap, hydraulic model study sites (two-letter codes, not referenced in this report), and the *Ceratonova shasta* infectious zone (thicker pink line).

Exposure duration for fish emigrating from the Shasta and Scott rivers were estimated separately based on an extensive radio telemetry dataset for age 1+ hatchery Coho Salmon collected by Beeman et al. (2012). We relied on reach-specific annual median travel times reported for the four years of the Beeman et al. (2012) study (2006-2009) to estimate median migration rates for fish emigrating from the Shasta River to Seiad and from the Scott River to Seiad. Given a high occurrence of low or zero weekly estimates of age 1+ Coho Salmon at the outmigrant trapping stations on both the Shasta and Scott rivers, we combined age 0+ and age 1+ fish for each population in the subsequent analyses.

Mortality Risk Data

Extended sentinel trials were designed to expose Coho and Chinook salmon to temporally variable *C. shasta* doses and temperatures to assess how these variables are associated with survival. Consequently, trials were conducted in multiple year-month combinations to capture responses over a range of parasite density and temperature combinations. All trials were conducted with fish enclosed in live-cages. The cages were placed in the mainstem just upstream of the confluence of the Klamath River with Beaver Creek (river kilometer 265). All *C. shasta* dose and temperature trial combinations also included 1-, 3-, 5- and 7-day exposures to estimate how survival may additionally be impacted by exposure duration. Groups assigned to 1-day treatments were removed after 24 hrs in-situ, 3 day treatments after 72 hrs, and so on. For all trials, groups were placed in cages on day-0 alongside an automated water sampler (hereafter termed ISCO; Teledyne, Lincoln NE).

Iron Gate hatchery production issues limited juvenile Coho availability among age classes for the two years (2014, 2015) of this data collection, hence the extended sentinel trials include both 0+ and 1+ age classes. Therefore, this modeling effort carries the assumption that the effects of covariates on mortality risk do not differ between age 0+ and 1+ juvenile Coho Salmon age classes. Previous work has found that juvenile fish size does not affect *C. shasta* infection in other susceptible salmonids (i.e., O. mykiss) (Bjork and Bartholomew 2009).

Post-exposure, fish were transported to the John L. Fryer Aquatic Animal Health Laboratory (AAHL), Corvallis, Oregon and held in specific-pathogen-free flow-through well water at a water temperature similar to the river water temperature during exposure. However, if river water temperatures averaged greater than 18 °C during the exposure period, the fish were maintained at temperatures at or less than 18 °C post-exposure because higher water temperatures, such as 20 - 22 °C, can make infections of the bacterium *Flavobacterium columnare* (the cause of columnaris disease) difficult to prevent. During the last hour of transport, the fish were given a 1 - 2 µg/mL Furan 2 (nitrofurazone) bath in their transport containers to prevent columnaris disease. In addition, within 1 - 2 weeks of their arrival at the AAHL, all fish were treated with formalin baths and oxytetracycline (TM 200) medicated food to prevent external parasites and bacterial infections. Control groups of each fish stock not exposed at the Klamath River sites were included for each monthly exposure and given the same preventative treatments as the river exposed fish. All groups of fish were monitored daily for *C. shasta* clinical disease signs for 2 months (in accordance with ACUP #5010). Moribund fishes were euthanized and examined microscopically for *C. shasta*-infection by wet mounts of lower gut material; if no myxospores were observed, intestinal samples were collected for *C. shasta*-PCR assays. A subsample of moribund fish from each group was also necropsied for other parasite and bacterial infections to eliminate those as causes of death and a subsample of visually positive (myxospores observed) samples were assayed by PCR to confirm visual results. For the purposes of this modeling effort, mortalities represent total fish loss with *C. shasta*-infections determined microscopically or by PCR testing from fish that died later than 5 days after they were brought to the AAHL.

To measure dose of *C. shasta* parasite over the exposure periods, water samples (1 L) were collected at 2-hr intervals and combined into a 12 L composite every 24-hrs by ISCO deployed adjacent to live-cages. Four 1 L subsamples were collected from each composite and filtered (5um, Millipore, Sigma-Aldrich, CA). DNA was extracted from 3 of the 4 subsampled liters using a Qiagen DNeasy kit (Hallett et al. 2012), and assayed to determine total *C. shasta* density (spores L-1) using a duplex *C. shasta*/IPC assay to enable simultaneous detection of *C. shasta* DNA and assessment of inhibition using the ABI Internal Positive Control. Controls were included in each qPCR run: positive (known numbers of spores) and negative (same buffer used for diluting the samples). Each run also included a reference dilution series of *C. shasta* DNA, for standard curve calibration and assay efficiency assessment. To quantify *C. shasta* genotype II specifically (for assessing risk to Coho), we employed a quantitative PCR assay to target a DNA sequence found only in genotype II from infected coho (differs from the above assay for total *C. shasta*, SYTO9 as the fluorescent reporter).

Model Development

We applied the binomial cure-rate component of the mixture – cure rate model of Ray et al. (2014) to the data from the extended sentinel trials. Input variables included exposure duration, average type-II (TII, known Coho Salmon specific genotype) spore concentration (spores/liter, s/L) over the exposure period, average Klamath River water temperature over the exposure period, and the rearing temperature of the laboratory holding tanks in which the experimental fish were stored. For this analysis, only the proportion of individuals dying from *C. shasta* is required, and we report and apply that component of the mixture cure model herein. To estimate how the probability of survival is associated with the suite of variables considered in this analysis, we fit a binomial generalized linear mixed-effects model (GLMM) with a logit link function. GLMM modeling extends standard regression by allowing for both fixed and random effects to account for variation in measured response variables (Hosmer and Lemshow 2013). For this model, we left open the possibility to include a random effect to account for over dispersion, which is a common issue for ecological data (Wu et al. 2015), should model goodness-of-fit testing deem it necessary. Fixed effects included the suite of variables discussed above, and potential interactive terms among the variables. In order to evaluate the statistical evidence for retaining interaction terms, we first considered a full model consisting of all main effects and all possible 2-way interactions among those variables. We then fit a set of *a priori* reduced models that included fewer numbers of the 2-way interactions. For each model we calculated the Watanabe-Akaike information criterion (WAIC), which is a suitable model selection metric for Bayesian models (Hooten and Hobbs 2015). Before proceeding, we opted to summarize for inference and make predications using the simplest model having a WAIC value less than 4 units away from the lowest WAIC scoring model.

We constructed the likelihood and specified prior distributions using BUGS language, and called JAGS (Plummer 2014) from R via the package jagsUI (Kellner 2014) to use Markov-Chain Monte Carlo (MCMC) simulation to draw samples from the joint posterior distribution of the parameters. Prior to drawing posterior samples, all continuous covariates were centered and scaled for numeric stability. Mean-zero Gaussian priors with precision (i.e., inverse variance) values of 0.001 were selected as noninformative priors for all regression coefficients, and a uniform (alpha, beta) prior (Gelman 2006) with alpha = 0 and beta = 100 was selected as a noninformative prior for the standard deviation of the random effects distribution.

For each model fit, we ran three simultaneous MCMC chains and retained 3000 samples per chain after a burn-in period of 5000 samples and a thinning rate of 50, which lead to the retainment of 9000 samples per parameter to be summarized for inference. Convergence of MCMC chains was assessed visually from traceplots of each MCMC chain, and quantitatively via the Gelman-Ruban convergence statistic (Rhat, Gelman et al. 2014). Model goodness-of-fit was assessed via posterior predictive checks, also called Bayesian p-values, which compare a goodness-of-fit metric computed across the MCMC samples of parameters for a chosen model and dataset with the same metric computed from an ideal dataset simulated directly from the chosen model. We selected the deviance as our goodness-of-fit metric, which is a common metric for GLMMs and suitable for grouped binomial data (Kery and Schaub 2012).

Altering Spore Concentration Response to Environmental Flows

Resource managers develop and implement environmental flow regimes to mitigate for the detrimental impacts of dams and water diversions on river form and ecological functions (Shea et al. 2016). Environmental flows are often constructed to mimic components of natural flow regimes such as the magnitude, frequency, duration, timing, variability, and sequencing of high and low flow events (Arthington et al. 2006). Environmental flows can target biological or physical objectives such as providing and maintaining aquatic habitat availability, flushing of accumulated sediments, maintaining a sediment balance, remobilization of gravels and formation of bars, scouring of vegetation, overtopping riverbanks with flow and sediment to augment floodplain development, etc. (Whiting 2002).

Environmental flow releases from Iron Gate Dam have recently been implemented by managers to disrupt the complex lifecycle of the myxozoan parasite *C. shasta.* The goal of these releases is to lower infection rates in outmigrating populations of juvenile Chinook and Coho Salmon in response to adversely affecting the habitat for *M. speciosa* , the parasite's alternate host (Alexander et al. 2016, Som et al. 2016a). In response to a formal request for technical assistance by NOAA Fisheries, we simulated the potential effects of environmental flow events on disease risk by conducting a series of POM estimates for the period of record for which we have spore concentration data (2005-2016).

Over approximately the last 15 years, there have been monitoring programs in place to concurrently collect data regarding water temperatures, weekly spore concentrations (total s/L and not necessarily TII), weekly *C. shasta* infection prevalence for Chinook Salmon, and weekly juvenile salmonid abundance estimates, with the later three occurring during the outmigration season. Over the same period, weekly-stratified TII s/L was directly measured in some weeks of the historic record considered for this analysis, and during many other weeks the proportion of total spore concentrations consisting of TII spores was measured. For weeks where the proportion of TII was measured we simply retained those weeks' proportion of the total spore values. For weeks where genotype proportion information was not available, we applied the annual average from that year's genotypic proportion sampling occurring during the spring and early summer period. In 2005, no genotype specific information was available, and so we applied 29% (which is the average of all within-year averages) of the total spore concentrations for all weeks. In 2015, the highest total s/L, for all genotypes combined and type I (TI, Chinook specific genotype), in the period of record were observed, and it was discovered that when TI spore concentrations are an extremely high proportion of the total spores (approximately 95%), they can mask the detection of TII spores. Hence, in 2015 a blanket proportion of 0.05 was applied to obtain TII s/L values for all weeks.

In the simulations, we altered the concentrations of TII s/L according to estimated decreases in the density of polychaete worms in monitoring data (Bartholomew et al. 2018) that resulted from environmental flushing events (described by Shea et al. 2016) and the Tribal Disease Technical Advisory Team (2017). There has only been a single year (2018), in which the polychaete index sampling was altered to capture potential changes in polychaete density that resulted from a 3-day, 6030 cfs surface flushing environmental flow targeted by a Federal District Court Order, and that environmental conditions allowed the sampling to commence as planned. In several recent years, attempts were made to alter the sampling schedule to more specifically capture the effects of other environmental discharge events, but water clarity and safety issues hampered the ability of samplers to effectively collect the required data. There were other years in which index polychaete sampling occurred and flows of this targeted magnitude and duration were reached, or approached, but in none of the other years of study did the combination of before and after sampling exist in ways to directly attribute observed changes to the flow event.

In the 2018 polychaete study, samples were collected from the three upper-most index sites roughly a month before the flushing flow event (3/1), immediately after the flow event (4/15), and a month after the flow event (5/15). It should be noted that these index samples are collected on boulder substrates, which are much more stable than cobble, gravel, and sand/silt substrates. At all three sites the density of polychaetes was dramatically reduced immediately after the flushing flow event, with densities ranging from 6% to 19% of their pre-event levels. A month later, densities had increased to between 15% and 25% of the pre-event levels, which still represents substantial decreases relative to estimated densities before the flow events. To reflect this potential level of change, a reduction of 75% of observed s/L was applied in the simulations. Given that these values relate to a single event as evidence, a conservative reduction to 25% of observed s/L values was also applied to the historic record of s/L to simulate potential reductions due to the more frequent flushing flow events. Further, in a previous analysis (BOR 2018) it was shown that the detection of s/L values above zero occurred roughly a month after flows on the descending limb of a spring hydrograph drop below 6000, with the potential for dryer years to see this time span shortened to roughly 3 weeks. To incorporate this observed phenomenon, we relied on the timing of the flushing flow events provided by the Bureau of Reclamation and later presented in their Final Biological Assessment on Klamath water operations (BOR 2018) to calculate delay in the simulated onset of s/L values exceeding zero. Finally, because the years 2005, 2006, and 2016 had springtime flows meeting or exceeding the magnitude and duration of the flushing flows, the methods discussed here were applied only to the timing of s/L becoming greater than zero in those years, but the proportional change in s/L was not applied for these three years.

In addition to altering the spore concentrations as described above, the flow management alternatives are also predicted to lead to water temperature regimes that differ from those historically observed. Prior to applying the POM model presented in this report, the RBM10 (Perry et al. 2011) water temperature model was applied to predict the water temperatures associated with the flow management alternative presented by BOR (2018). All POM predictions provided below are computed using water temperatures generated with the RBM10 model.

It is the standard practice of the Arcata Fish and Aquatic Conservation Program and other authors of this document to include measures of precision (e.g., confidence intervals) with any statistical estimates that are generated. In the present analysis, the California Department of Fish and Wildlife's weekly abundance estimates, predicted percent mortalities generated by the statistical model described above, TII s/L values, modeled temperatures, and exposure durations of the Shasta and Scott fish are all among the list of items prone to prediction or measurement error. At this time, we have only the precision related to the statistical model described above, and because of our imposed value of 0 predicted percent mortality when TII s/L is less than 1, estimates of that precision are unknown. Hence, at this time we do not report confidence intervals for the POM values, but plan to explore suitable methods to incorporate important sources of error in future iterations of this analysis. This analysis also does not include production of Coho Salmon from Bogus Creek, which has been monitored by the CDFW since 2015. As Bogus Creek can be a significant source of Coho Salmon to the mainstem Klamath River, we are also looking to incorporate Coho Salmon from Bogus Creek into future analyses.

Results

Travel Times and Statistical Model

For simulating travel times through the infectious zone, we selected the highest annual median exposure time of 2.42 d calculated for 2006 (Beeman et al. 2012) for Shasta River migrants (Table 1). We used a 1-d exposure time for age 0+ and age 1+ Coho Salmon migrating between the Scott River confluence and Seiad given that was the lowest data point in the extended sentinel trials (1, 3, 5, and 7 days). The exposure durations we used are conservative given they are based on travel times observed for age 1+ fish from the Beeman et al. (2012) study, and average travel times for combined age 1+ and age 0+ fish will likely be much longer because age 0+ migrate more slowly than age 1+ Coho Salmon (Manhard et al. 2018).

Initial model fitting revealed Bayesian p-values approaching 1, which is a clear indication of overdispersion, and therefore only models accounting for overdispersion, via a random effect allowing for extra-binomial variation at the experimental cage level, were considered as candidate models. Although there was some evidence that several of the candidate models including multiple interaction terms could be used for inference, the model meeting our *a priori* criteria of being the simplest model with 4 WAIC units of the best fitting model was the model containing only an interaction of the exposure and rearing temperatures (Table 2). Further, there was no evidence that overdispersion remained an issue for the selected model that included the random effect noted above (Bayesian p-value = 0.67).

Table 1. Median reach-specific travel times and migration rates of hatchery Coho Salmon in the mainstem Klamath River between the confluence of the Shasta River and Indian Creek (Beeman et al. 2012) used to calculate exposure duration of Coho Salmon in the Shasta to Seiad and Scott to Seiad reaches.

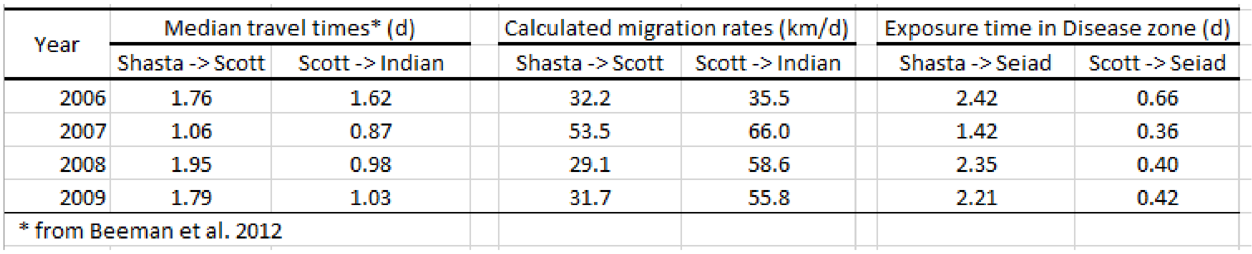

Year	Median travel times* (d)		Calculated migration rates (km/d)		Exposure time in Disease zone (d)	
	Shasta -> Scott	Scott -> Indian	Shasta -> Scott	Scott -> Indian	Shasta -> Seiad	Scott -> Seiad
2006	1.76	1.62	32.2	35.5	2.42	0.66
2007	1.06	0.87	53.5	66.0	1.42	0.36
2008	1.95	0.98	29.1	58.6	2.35	0.40
2009	1.79	1.03	31.7	55.8	2.21	0.42

* from Beeman et al. 2012

Table 2. Candidate models ranked by WAIC values. Abbreviations are as follows: spore concentrations (sL), exposure temperature (eT), rearing temperature (rT), exposure duration (eD).

Model Name	Interaction Terms	WAIC	ΔWAIC
Full	sL*eT; sL*rT; sL*eD; eT*rT; eT*eD; rT*eD	106.8	
R0	sL*eT; sL*rT; sL*eD; eT*rT; eT*eD	108.2	1.4
R1	sL*eT; sL*eD; eT*rT; eT*eD	108.2	1.4
R2	sL*eD; eT*rT; eT*eD	111.2	4.4
R3	eT*rT; eT*eD	109.7	2.9
R4	eT*rT	110.7	3.9

The selected model matches the observed data very well, with a linear correlation between model-predicted probabilities of survival and the observed data from the extended sentinel trials equaling 0.93 (Figure 2). Further, there is strong evidence that the variables in the selected model are associated with the probability of *C. shasta* mortality (Table 3). As expected, increasing spore concentrations (Figure 3) and exposure durations (Figure 4) are associated with decreasing survival. The exposure and rearing temperatures are also associated with *C. shasta* mortality, but given their interactive effects in this model, it is most appropriate to discuss their effects in concert. For instance, at relatively cool rearing temperatures, increasing exposure temperatures are predicted to dramatically reduce survival, but this effect is muted for warmer rearing temperatures (Figure 5). This result makes sense given the way the exposure and rearing periods played out, in that exposure periods between one and seven days are much shorter than the rearing period, which can last several months for individuals that do not die from ceratomyxosis. At warmer rearing temperatures that last for several months, it makes sense that additional effects due to the temperature during a shorter, initial, exposure periods would be lessened. This interactive behavior also highlights the need to avoid extrapolation beyond ranges of the data observed in this study when applying the model to predict mortality response in naturally migrating fish of the Klamath River. As such, all predictions provided below are constructed with variables values that have been constrained within the minimum and maximum values of each respective variable from the data set used to fit the statistical model and estimate parameters.

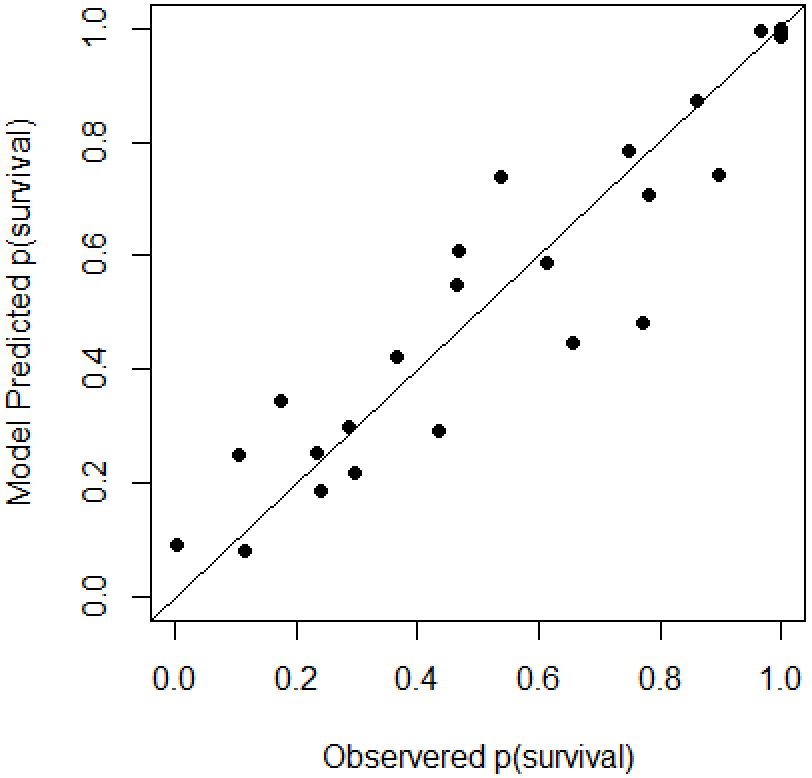

Figure 2. The model-predicted, computed using the posterior means of all estimated model parameters, probability of survival for each extended sentinel trial plotted against the observed probability of survival from each trial. The line is a 1-to-1 line representing perfect agreement between the predicted and observed values.

Table 3. Estimated coefficients from selected model. Values in the Estimate column were generated by calculating the mean value over all posterior distribution values for each coefficient, and the 95% credible interval values were generating by calculating the 0.025 and 0.975 percentiles over all posterior distribution values for each coefficient. "p(non-zero)" is the probability that a coefficient is non-zero, and can be used to assess the strength of evidence that a coefficient is correlated with the response value. All values in this table are on the logit scale.

	Estimate	Lower 95%	Upper 95%	p(non-zero)
Intercept	0.18	-0.35	0.72	0.76
Spore Conc.	-0.73	-1.20	-0.31	>0.99
Exposure Temp.	-1.77	-2.66	-0.95	>0.99
Rearing Temp.	0.12	-0.59	0.82	0.64
Exposure Duration	-0.58	-1.00	-0.20	>0.99
Exp T. * Rear. T.	0.99	0.23	1.90	>0.99

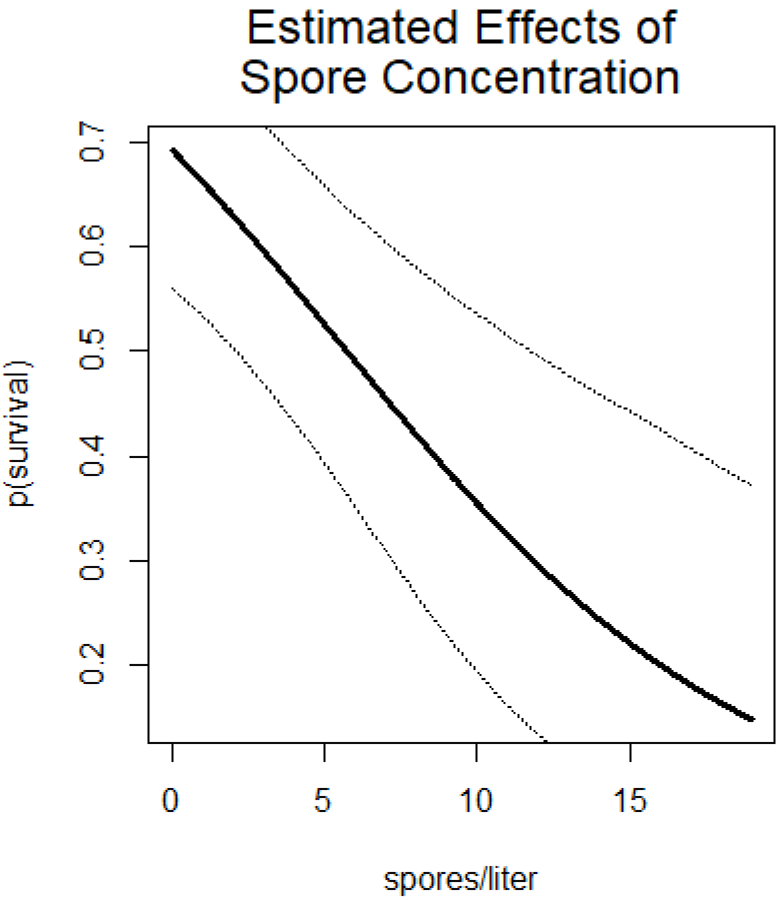

Figure 3. The estimated effects (solid line, computed as mean of posterior distribution) of spore concentration on the probability of survival, and 95% credible intervals (dotted line). For this figure, exposure temperature, rearing temperature, and exposure duration were held at their average values.

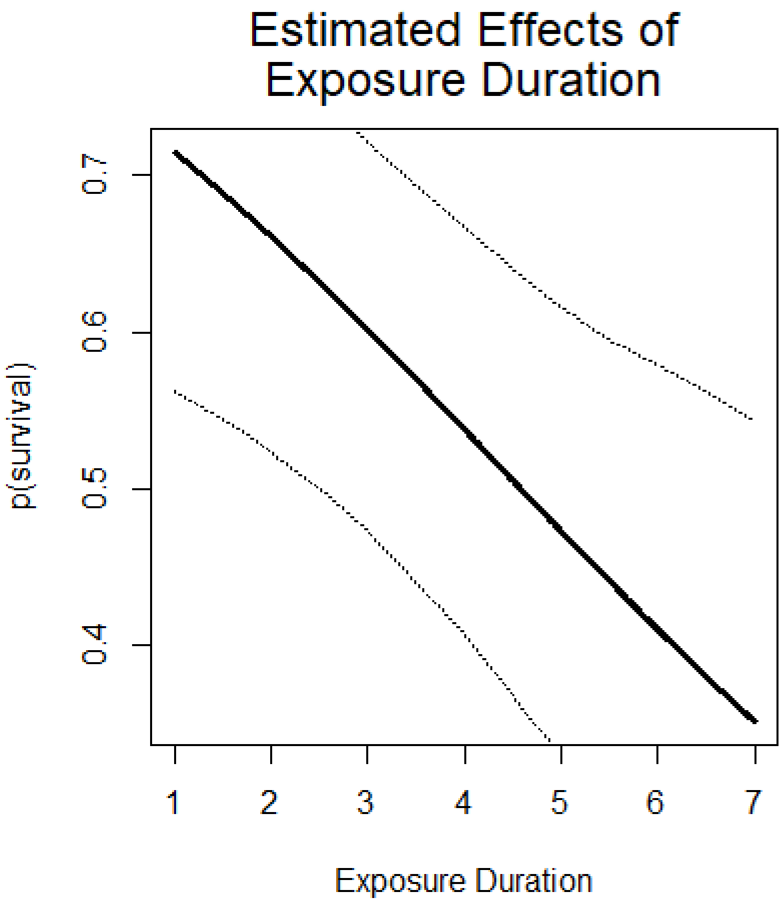

Figure 4. The estimated effects (solid lines, computed as means of posterior distributions) of exposure duration on the probability of survival, and 95% credible intervals (dotted lines). For this figure, rearing temperature, exposure temperature, and spore concentration were held at their average values. The units on exposure duration is days.

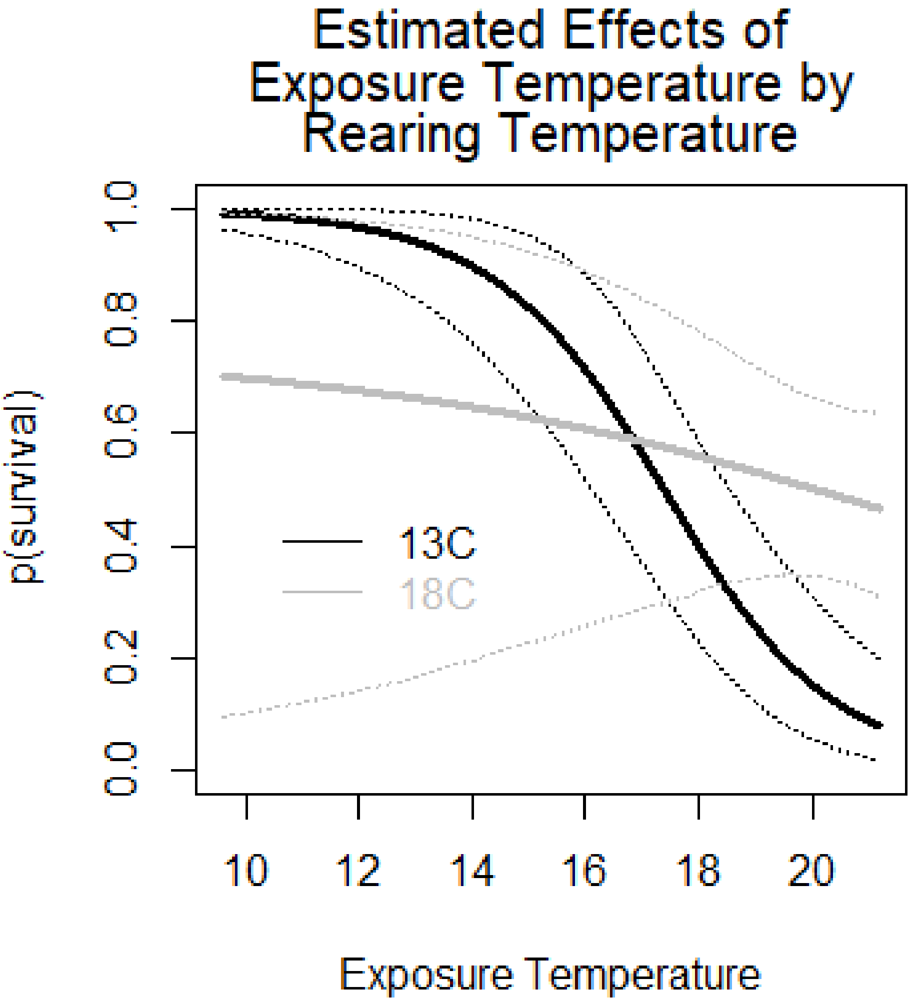

Figure 5. The estimated effects (solid lines, computed as means of posterior distributions) of exposure temperature on the probability of survival, and 95% credible intervals (dotted lines), for a relatively cool rearing temperature (13C, black lines), and a relatively warm rearing temperature (18C, gray lines). For this figure, spore concentrations and exposure duration were held at their average values.

Simulating Coho Salmon Response to Environmental Flows

The 25% and 75% reductions in spore concentration associated with the flow management alternatives are each predicted to result in lower levels of annual mortality due to *C. shasta* (Table 4). Variation among years between the two migration corridors can be generally attributed to differing spore concentration and temperatures. Additional inter-annual variation was influenced by the match or mismatch of timing between fish migration and waterborne spore concentrations. It may appear strange that the predicted POM values are predicted to increase for water year 2005 with a 25% reduction in spore concentration. However, it is important to note that in 2005 there was a long period of elevated discharge that lasted much of the month of May. The flow management alternatives include flushing flow events that occur earlier in the year, and hence the period-of-record hydrology simulations do not contain the May event for 2005. In the simulations, May discharges are much lower than experienced historically, and the resulting predictions of spore concentrations and water temperatures during the month of May lead to modest amounts of disease risk.

Table 4. Predicted prevalence of mortality of age 0+ and age 1+ (combined) Coho Salmon in the mainstem Klamath River between the Shasta River confluence and Seiad (top, 2.42 day exposure length) and the Scott River confluence and Seiad (bottom, 1 day exposure length). Predictions are provided for spore concentration and temperature values as they have been monitored ("Historic"), and also for two hypothesized ways that spore concentrations may be altered via proposed flow management that include both a 25% and 75% reduction in spore concentrations ("25% red." and "75% red.", respectively).

Shasta River to Seiad

Year	Historic	25% red.	75% red.
2005	0	0.047	0
2006	0.03	0.031	0.019
2007	0.378	0.326	0.209
2008	0.678	0.604	0.382
2009	0.229	0.168	0.098
2010	0.017	0	0
2011	0	0	0
2012	0	0	0
2013	0	0	0
2014	0.413	0.347	0.152
2015	0.263	0.179	0.07
2016	0.092	0	0

Scott River to Seiad

Year	Historic	25% red.	75% red.
2005	0	0.154	0
2006	0.12	0.176	0.092
2007	0.135	0.109	0.059
2008	0.603	0.557	0.327
2009	0.019	0.013	0.007
2010	0.002	0	0
2011	0	0	0
2012	0	0	0
2013	0	0	0
2014	0.245	0.145	0.04
2015	0.133	0.124	0.05
2016	0.004	0	0

Literature Cited

Alexander, J. D., J. L. Bartholomew, K. A. Wright, N. A. Som, and N. J. Hetrick. 2016. Integrating models to predict distribution of the invertebrate host of myxosporean parasites. Freshwater Science. Online Early. doi: 10.1086/688342.

Arthington, A.H., S.E. Bunn, N.L. Poff, and R.J. Naiman. 2006. The challenge of providing environmental flow rules to sustain river ecosystems. Ecological Applications 16(4)-1311-1318.

Bartholomew, J. L. 1998. Host resistance to infection by the mxyosporean parasite *Ceratomyxa shasta*: A review. Journal of Aquatic Animal Health: 10:112-120.

Bartholomew, J. L., M. J. Whipple, and D. Campton. 2001. Inheritance of resistance to *Ceratomyxa shasta* in progeny from crosses between high- and low-susceptibility strains of rainbow trout (*Oncorhynchus mykiss*). Bulletin of the National Research Institute of Aquaculture. Supplement 5:71-75.

Bartholomew, J., S. Hallett, R. Holt, J. Alexander, S. Atkinson, R. Craig, A. Javaheri, and M. Babbar-Sebens. 2018. Klamath River Fish Health Studies: Salmon Disease Monitoring and Research Interagency Agreement #R15PG00065 Annual Report April 2017 – March 2018. Oregon State University, Corvallis, Oregon.

Beeman, J., Juhnke, S., Stutzer, G., and Wright, K. 2012. Effects of Iron Gate Dam discharge and other factors on the survival and migration of juvenile coho salmon in the lower Klamath River, northern California, 2006–09: U.S. Geological Survey Open-File Report 2012-1067, 96 p.

Bjork S. J., and J. L. Bartholomew. 2009. Effects of *Ceratomyxa shasta* dose on a susceptible strain of rainbow trout and comparatively resistant Chinook and coho Salmon. Diseases of Aquatic Organisms 86:29–37. doi: 10.3354/dao02092.

Bureau of Reclamation (BOR) 2018. U.S. Bureau of Reclamation Hydrologic Assessment Relative to Court Injunction. United States District Court for Northern District of California San Francisco Division Case 3:16-cv-04294-WHO Document 144-2 Filed 03/27/18.

Bureau of Reclamation (BOR). 2018. The Effects of the Proposed Action to Operate the Klamath Project from April 1, 2019 through March 31, 2029 on Federally-Listed Threatened and Endangered Species. Final Biological Assessment.

Chesney, D. and M. Knechtle. 2016. Shasta River Chinook and Coho Salmon Observations in 2015, Siskiyou County, CA. Final Report, Klamath River Project. California Department of Fish and Wildlife.

Ching, H. L., and D. R. Munday. 1984. Geographic and seasonal distribution of the infectious stage of *Ceratomyxa shasta* Noble, 1950, a myxozoan salmonid pathogen in the Frazer River system. Canadian Journal of Zoology 62:1423–1424.

Disease Technical Advisory Team (D. Hillemier, M. Belchick, T. Soto, C. Tucker, and S. Ledwin). 2017. Measures to reduce *Ceratonova shasta* infection in Klamath River Salmonids: A Guidance Document. January 17, 2017.

Esch, G. W., and Fernandez, J. C. 1993. Evolutionary Aspects. pp. 231-267 in: A Functional Biology of Parasitism: Ecological and Evolutionary Implications. Chapman and Hall, London.

Fujiwara, M., M. S. Mohr, A. Greenberg, J. S. Foott, and J. L. Bartholomew. 2011. Effects of ceratomyxosis on population dynamics of Klamath fall-run Chinook salmon. Transactions of the American Fisheries Society 140:1380–1391.

Gelman, A. 2006. Prior distributions for variance parameters in hierarchical models (comment on article by Browne and Draper). Bayesian Anal. 1(3): 515–534. doi:10.1214/06-BA117A.

Gelman, A., Carlin, J.B., Stern, H.S., Dunson, D.B., Vehtari, A., and D. B. Rubin. 2014. Bayesian data analysis. 3rd ed. CRC Press, Boca Raton, Fla.

Hallett, S. L., R. A. Ray, C. N. Hurst, R. A. Holt, G. R. Buckles, S. D. Atkinson, and J. L. Bartholomew. 2012. Density of the waterborne parasite *Ceratomyxa Shasta* and its biological effects on salmon. Applied and Environmental Microbiology 78:3724—3731. doi: 10.1128/AEM.07801-11.

Hooten, M.B, and Hobbs, N.T. 2015. A guide to Bayesian model selection for ecologists. Ecological Monographs 85(1): 3-28. doi:10.1890/14-0661.1.

Hosmer, D.W., Jr., Lemeshow, S., and Sturdivant, R.X. 2013. Applied logistic regression. 3rd ed. John Wiley & Sons, Inc., Hoboken, N.J.

Kery, M., and Schaub, M. 2012. Bayesian Population Analysis Using WinBUGS. Academic Press, Oxford, UK.

Manhard, C. V., N. A. Som, R. W. Perry, J. R. Faukner, and T. Soto. 2018. Estimating freshwater productivity, overwinter survival, and migration patterns of Klamath River Coho Salmon. U.S. Fish and Wildlife Service. Arcata Fish and Wildlife Office, Arcata Fisheries Technical Report Number TR 2018-33, Arcata, California.

Perry, R.W., Risley, J.C., Brewer, S.J., Jones, E.C., and Rondorf, D.W., 2011, Simulating daily water temperatures of the Klamath River under dam removal and climate change scenarios: U.S. Geological Survey Open-File Report 2011–1243, 78 p.

Ray, R. A., R. W. Perry, N. A. Som, and J. L. Bartholomew. 2014. Using Cure Models for Analyzing the Influence of Pathogens on Salmon Survival. Transactions of the American Fisheries Society, 143(2), 387-398. doi:10.1080/00028487.2013.862183.

Shea, C., N. J. Hetrick, and N. A. Som. 2016. Response to Request for Technical Assistance – Sediment Mobilization and Flow History in Klamath River below Iron Gate Dam. Arcata Fish and Wildlife Office Technical Memorandum. Arcata, California.

Som, N. A., N. J. Hetrick, and J. Alexander. 2016a. Response to Request for Technical Assistance – Polychaete Distribution and Infections. Arcata Fish and Wildlife Office Technical Memorandum. Arcata, California.

Som, N. A., N. J. Hetrick, J. S. Foott, and K. True. 2016b. Response to Request for Technical Assistance – Prevalence of *C. shasta* infections in Juvenile and Adult Salmonds. Arcata Fish and Wildlife Office Technical Memorandum. Arcata, California.

Stone, R., J. S. Foott, and R. Fogerty. 2008. Comparative susceptibility to infection and disease from *Ceratomyxa shasta* and *Parvicapsula minibicornis* in Klamath River basin juvenile Chinook, coho and steelhead populations. U.S. Fish and Wildlife Service, California-Nevada Fish Health Center, Anderson, CA.

Toft, C. A., and A. Aeschlimann. 1991. Introduction: Coexistence or Conflict? pp. 1-12 *in* Parasite-Host Associations: Coexistence or Conflict? Oxford University Press. Oxford.

Thompson, J. N. (1994). The Coevolutionary Process. University of Chicago Press, Chicago.

True, K., A. Voss, and J. Foott. 2017. Myxosporean Parasite (*Ceratonova shasta* and *Parvicapsula minibicornis*) Prevalence of Infection in Klamath River Basin Juvenile Chinook Salmon, March – August 2017. U.S. Fish and Wildlife Service California – Nevada Fish Health Center, Anderson, California.

Webster, J. P., J. Shrivastava, P. Johnson, and L. Blair. 2007. Is host-schistosome coevolution going anywhere? BMC Evolutionary Biology, 7:91.

Whiting, P. J. 2002. Streamflow Necessary for Environmental Maintenance. Annual Review Earth and Planetary Science, 30:181-206.

Wu, G., Holan, S.H., Nilon, C.H., and Wikle, C.K. 2015. Bayesian binomial mixture models for estimating abundance in ecological monitoring studies. Ann. Appl. Stat. 9(1): 1-26. doi:10.1214/14-AOAS801.